Ecotoxicology and Environmental Safety 279 (2024) 116416

Contents lists available at ScienceDirect

Ecotoxicology and Environmental Safety

journal homepage: www.elsevier.com/locate/ecoenv

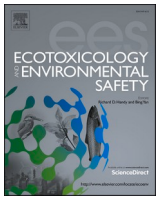

Contrasting plant-induced changes in heavy metals dynamics: Implications for phytoremediation strategies in estuarine wetlands

Amanda Duim Ferreira [a], Hermano Melo Queiroz [a], Alexys G. Friol Boim [a], Owen W. Duckworth [b], Xosé L. Otero [c], Ângelo Fraga Bernardino [d], Tiago Osório Ferreira [a,*]

[a] Department of Soil Science, "Luiz de Queiroz" College of Agriculture, University of São Paulo, Piracicaba, São Paulo, Brazil
[b] Crop and Soil Department. North Carolina State University, United States
[c] Departamento de Edafología y Química Agrícola, Facultad de Biología, Universidad de Santiago de Compostela, Spain
[d] Grupo de Ecologia Bentônica, Departamento de Oceanografia, Universidade Federal do Espírito Santo, Vitória, Espírito Santo, Brazil

ARTICLE INFO

Edited by Dr R Pereira

Keywords:
Metal biogeochemistry
Macrophytes
Sea hibiscus
Phytoextraction
Phytostabilization

ABSTRACT

Wetland plants play a crucial role in regulating soil geochemistry, influencing heavy metal (HM) speciation, bioavailability, and uptake, thus impacting phytoremediation potential. We hypothesized that variations in HM biogeochemistry within estuarine soils are controlled by distinct estuarine plant species. We evaluated the soils (pH, redox potential, rhizosphere pH, HM total concentration, and geochemical fractionation), plant parts (shoot and root), and iron plaques of three plants growing in an estuary affected by Fe-rich mine tailings. Though the integration of multiple plant and soil analysis, this work emphasizes the importance of considering geochemical pools of HM for predicting their fate. Apart from the predominance of HM associated with Fe oxides, *Typha domingensis* accumulated the highest Cr and Ni contents in their shoots ($>$ 100 mg kg^{-1}). In contrast, *Hibiscus tiliaceus* accumulated more Cu and Pb in their roots ($>$ 50 mg kg^{-1}). The differences in rhizosphere soil conditions and root bioturbation explained the different potentials between the plants by altering the soil dynamics and HM's bioavailability, ultimately affecting their uptake. This study suggests that *Eleocharis acutangula* is not suitable for phytoextraction or phytostabilization, whereas *Typha domingensis* shows potential for Cr and Ni phytoextraction. In addition, we first showed *Hibiscus tiliaceus* as a promising wood species for Cu and Pb phytostabilization.

1. Introduction

Estuarine soils are commonly impacted by heavy metals (HMs) because they may receive contaminant loads from upstream watersheds transported by rivers and accumulate within estuaries (Hadlich et al., 2018; Varzim et al., 2019). In estuarine ecosystems, HMs may have several fates: they may be retained and accumulated in the soils, absorbed by plants, released into estuarine waters, or concentrated in the tissues of aquatic organisms (De Luca Rebello et al., 1986). Thus, HMs may be transferred along the food chain, thus posing serious risks to human and environmental health (Gabriel et al., 2020a; Jiang et al., 2020).

In these environments, estuarine plants may differ in their impact on estuarine soil geochemistry (Enya et al., 2019; Yan et al., 2022), ultimately affecting HM bioavailability and, thus, the plant's ability to promote phytoremediation. The removal of HMs from soils can be influenced by various plant traits and plant-mediated soil processes, such as evapotranspiration (Schück and Greger, 2020a), biomass production (Zhang et al., 2019), root system architecture (Schück and Greger, 2020b), root uptake kinetics (Ao et al., 2022), translocation mechanisms (e.g., metal transporters; (Rascio and Navari-Izzo, 2011)). These processes alter soil geochemical conditions allowing plants to access HMs from the soil solution and other soil fractions. For example, plants may enhance the reductive dissolution of Fe (oxyhydr)oxides through the input of labile organic matter (e.g., root exudates), which may result in the concomitant release of mineral-associated HMs (Queiroz et al., 2021). In contrast, estuarine plants can control HM bioavailability by promoting metal precipitation in their rhizosphere (Li et al., 2019). Radial oxygen loss (ROL) through root pores can oxidize elements (e.g., As(III)) and potentially reduce their bioavailability (Li et al., 2019; Xue et al., 2022). ROL can also oxidize other elements (e.g., Fe and Mn) that control HM speciation through the formation of

* Correspondence to: Luiz de Queiroz College of Agriculture, University of São Paulo (ESALQ-USP), Av. Pádua Dias 11, Piracicaba, SP 13418-900, Brazil.
E-mail address: toferreira@usp.br (T.O. Ferreira).

https://doi.org/10.1016/j.ecoenv.2024.116416
Received 11 December 2023; Received in revised form 20 April 2024; Accepted 28 April 2024
Available online 15 May 2024

precipitates on the root surface (e.g., iron plaques, IP), which may act as barriers to (Zhang et al., 2023) or sources of HMs for plant uptake (Health et al., 2022; Zhang et al., 2022; Ferreira et al., 2022a).

In 2015, Brazil experienced its largest environmental disaster (i.e., Mariana's disaster; (Hatje et al., 2017)). The discharge of Fe mine tailings released 60 million tons of Fe-rich tailings into the Rio Doce Estuary, causing environmental impacts associated with HMs in soil, water, plants, and fauna (Ferreira et al., 2022a, 2022b; Bernardino et al., 2019; Queiroz et al., 2018; Gabriel et al., 2020b; Barcellos et al., 2022). Previous studies have revealed that iron (Fe) (oxyhydr)oxides present in tailings and impacted estuarine soils played key roles in HM bioavailability (Queiroz et al., 2021, 2018). Interestingly, a recent study identified the widespread colonization of Fe-rich mine tailings by different native estuarine plants (Queiroz et al., 2022). However, the impact of these plants on the chemistry of the soils and biogeochemical cycling HMs with them is currently unknown.

In the present study, we hypothesized that three native estuarine plants (*Typha domingensis*, *Eleocharis acutangula*, and *Hibiscus tiliaceus*) may exert contrasting effects on the dynamics, removal, and stabilization of HMs in estuarine soils affected by Fe-rich mine tailings. The present study aimed to assess the potential of three estuarine plants for HM phytoremediation and to determine the plant-mediated soil mechanisms used by each plant. To achieve these objectives, soil and plant samples were collected from three sites in the Rio Doce estuary—each colonized by a monospecific stand of each plant. The total content of chromium, cooper, lead and nickel in the soil and different plant compartments (i.e., shoot, root, and iron plaques (IPs)) were determined. Moreover, soil HM chemical partitioning was carried out to elucidate their geochemical behavior in soils with different plant covers.

2. Material and methods

2.1. Setting, sampling, and in situ measurements

The estuarine environment used as a framework (Fig. 1), known for its fishing communities, surfing, tourism, and environmental conservation activities, has been severely impacted by Fe-rich mine tailing depositions due to the rupture of the Fundão dam. In 2015, more than 50 million cubic meters of Fe mine tailings were released into the Rio Doce basin (Gabriel et al., 2020b; Barcellos et al., 2022). These mine tailings traveled more than 600 km, reaching the estuary 17 days later after the dam rupture (Bernardino et al., 2019). In addition, after the disaster, the total content of heavy metals such as Cr, Ni, Cu, and Pb in the estuarine sediments increased by 2–5 times (Gomes et al., 2017). In addition, Queiroz et al (Queiroz et al., 2018). reported that heavy metals in the recently deposited mine tailings in the estuary were associated with iron oxides, which could increase its ecological risks due to Fe reductive dissolution and associated metals release (Queiroz et al., 2021).

The region has two well-defined climate seasons: dry winter (April to September) and rainy summer (October to March; (Bernardino et al., 2015); Bissoli and Bernardino, 2018). In 2019 (four years after the initial tailing deposition), soil and plant samples were collected from three

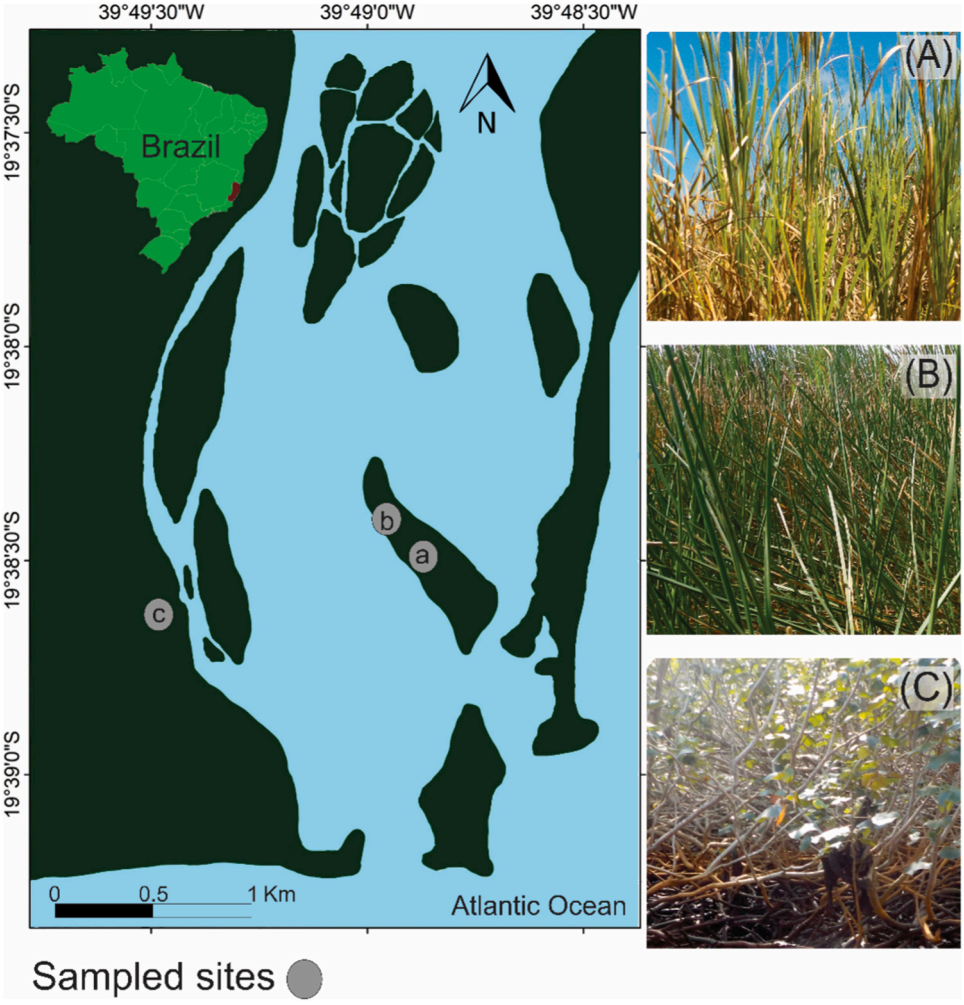

Fig. 1. Sampling locations at the *Rio Doce* estuary and images of the different plant species studied: (A) *Typha domingensis*, (B) *Eleocharis acutangula*, and (C) *Hibiscus tiliaceus*.

plots at three sites in the Rio Doce estuary (Fig. 1). Each area was colonized by a monospecific stand of estuarine plant species (i.e., *Typha domingensis*, *Eleocharis acutangula*, and *Hibiscus tiliaceus*) to evaluate their role in the geochemical behavior of HMs in the soil after the deposition of Fe-rich tailings. These plants were chosen for their representativeness in the estuarine environment, as they are the main native species naturally occurring in the Rio Doce estuary. Additionally, the use of native species in phytoremediation trials can be more effective due to the habitat adaptation of these species (Fadzil et al., 2023), especially in wetland environments that require flooding adaptations.

Typha domingensis and *Eleocharis acutangula* are both monocot species native to South America, commonly found in tropical wetland ecosystems (Rosen et al., 2007). The plant species *T. domingensis* (Fig. 1A) belongs to the order Poales and it is a perennial, herbaceous plant with a dense root system and efficient propagation via seeds and rhizome (Paiva et al., 2020). Conversely, *E. acutangula* (Fig. 1B) has an underground rhizome, adventitious roots, and culms responsible for photosynthesis, with leaves serving as protective bracts (Baksh and Richards, 2006). On the other hand, *H. tiliaceus*, a perennial eudicot species native to coastal and near-coastal ecosystems from the Malvaceae family, is characterized by ovate to orbicular leaves and a spreading lateral root system (Verdcourt and Mwachala, 2009).

Samples of the aerial parts of *T. domingensis* and *E. acutangula* were collected using a 0.5 m × 0.5 m square plot. All biomass within this sampling area was harvested as near as possible from the soil surface. For *H. tiliaceus,* well-developed leaves were collected from the tree crown. Aerial biomass was washed with deionized water and dried in an oven at 65 °C until a constant weight was achieved. The biomass was crushed in a mill and stored in plastic bags until analysis.

Before the soil sampling, polyvinyl chloride tubes (PVC) were washed with 10 % HCl. At each sampling location (Fig. 1), three points were selected as replication sites. At each replication site, two soil cores were collected (Fig. S1), totaling six replications per plant species. Soil cores (40 cm long, with a 67 mm internal diameter) were collected in triplicate at the center of each plot (Fig. S1) using PVC tubes. After sampling, all cores were hermetically stored upright at 4 °C. Upon returning to the laboratory, the cores were sectioned at every 10 cm, and the soil samples were stored in plastic bags in the dark at 4 °C until analysis.

Bulk soil pH and redox potentials (Eh) were measured in the field using portable pH and ORP meters (Hanna®, model HI-991002) (Fig. S2). The pH glass electrode was previously calibrated with standard solutions (pH 4.0 and 7.0). At the same time, the Eh values were recorded using a platinum electrode, and the obtained values were corrected by adding the value for the calomel reference electrode (+244 mV).

2.2. Soil characterization

Soil total organic carbon (TOC) and particle size distribution were determined from samples at each site (Table 1). Before TOC determination, inorganic carbon was removed using 1 mol L^{-1} HCl. Then, TOC was determined using an elemental analyzer (LECO 144 SE-DR) (Howard et al., 2014). Particle size distribution (Table 1) was determined according to Stokes' law after removing organic matter and carbonates from the soils (Gee and Bauder, 1986).

The soil total contents of HMs (Cr, Cu, Ni, and Pb) were obtained after acid digestion using the USEPA method 3052 (United States Environmental Protection Agency, 1996). A soil-certified material (NIST - San Joaquin Soil 2709a) was digested using the same protocol as the samples to verify reliability (Supplementary Information Table S1).

Additionally, sequential extraction was performed to obtain six operationally different fractions to determine HMs concentrations associated with varying fractions of soil, according to the methodologies proposed by (Ferreira et al., 2007) and (Otero et al., 2009). Briefly:

EX – Exchangeable HMs: 2.0 g were stirred for 30 min in 30 ml of 1 mol L^{-1} $MgCl_2$ solution (pH 7.0).

CA – HMs associated with carbonates were stirred for 5 h in 30 ml of 1 mol L^{-1} NaOAc solution (pH 5.0).

SRO – HMs associated with short-range Fe oxide: stirred for six h at 96 °C in 30 ml of hydroxylamine solution 0.04 mol L^{-1} + 25 % acetic acid (v/v) solution.

CO– HMs associated with crystalline Fe oxides: stirred for 30 min at 75 °C in 20 ml of 0.25 mol L^{-1} sodium citrate + 0.11 mol L^{-1} sodium bicarbonate with 3 g of sodium dithionite.

Before the next fraction extraction, silicates were removed by stirring samples with 30 ml of HF 10 mol L^{-1} for 16 h at room temperature. Then, at room temperature, organic matter was removed by stirring samples with 15 ml of concentrated sulfuric acid for two h.

PY – HMs associated with pyrite: stirred for two h at room temperature with 10 ml of concentrated HNO_3.

The easily available (EA) fraction was considered the sum of EX and CA contents (Li et al., 2019; Ren et al., 2015).

Table 1
Total organic carbon contents (TOC) and particle size distribution of the soils collected at the study's three sites in the *Rio Doce* estuary, Brazil.

Site	Plant species	Depth (cm)	TOC %	Clay	Silt	Sand
1	*T. domingensis*	0–10	1.4 ± 0.0	19.2 ± 9.5	24.3 ± 18.4	19.2 ± 9.5
		10–20	1.7 ± 0.1	43.6 ± 1.5	44.8 ± 2.8	11.6 ± 3.9
		20–30	0.9 ± 0.2	24.3 ± 5.2	20.1 ± 12.9	55.6 ± 10.9
		30–40	0.2 ± 0.2	1.3 ± 0.0	1.7 ± 0.0	97 ± 0.0
2	*E. acutangula*	0–10	2.3 ± 1.0	24.3 ± 10.2	36.9 ± 6.4	38.8 ± 16.5
		10–20	1.8 ± 0.6	41 ± 5.3	44.6 ± 3.1	14.3 ± 8.4
		20–30	0.8 ± 0.9	20.9 ± 8.8	18.6 ± 14.7	60.4 ± 18.8
		30–40	0.1 ± 0.0	1.3 ± 0.0	1.7 ± 0.0	97 ± 0.0
3	*H. tiliaceus*	0–10	3.1 ± 0.2	40.4 ± 4.0	46.8 ± 4.0	12.9 ± 3.3
		10–20	2.2 ± 0.4	40.3 ± 4.2	51.4 ± 4.6	8.4 ± 1.4
		20–30	1.9 ± 0.0	44.8 ± 6.0	46.8 ± 5.1	8.4 ± 2.6
		30–40	2.5± 0.3	44.4 ± 13.0	48.1 ± 10.7	7.5 ± 2.5

2.3. Roots and rhizosphere soil collection

At each soil depth (i.e., 10 cm), the roots were carefully selected and vigorously shaken to remove loose soil. The soil firmly adhered to the roots (operationally defined as rhizosphere soil; Edwards et al., 2015) and was collected by brushing the roots (Edwards et al., 2015). After collecting the rhizosphere soil, roots were washed repeatedly with deionized water and then stored at 4 ºC.

2.4. Determination of rhizosphere pH

Rhizosphere soil was incubated for 1 h with deionized water (1 g of soil: 2.5 ml of water) at room temperature, and then, the pH of the rhizosphere soil (rhz-pH) was measured (Jackson, 1998) using a pH meter (Digimed®, DM-22 model) previously calibrated with standard solutions (pH 4.0 and 7.0).

2.5. Iron plaques extraction and plant parts acid digestion

For root IP extraction, 1.0 g samples of washed roots were weighed and immersed in a solution containing 40 ml of 0.3 mol L^{-1} sodium

citrate, 5 ml of 1.0 M sodium bicarbonate, and 1.0 g sodium dithionite. The samples were mechanically shaken on a horizontal shaker at 125 rpm for 16 h at room temperature (Taylor and Crowder, 1983) (Fig. S3). The extracts were stored frozen (< 4 ºC) until analysis. Then, roots were repeatedly washed with deionized water and placed in an oven at 65 °C to dry until constant weight.

Roots and aerial biomass were digested using the USEPA method 3050 B (USEPA, 2007). Certified material from strawberry leaves (LGC 7162) and duplicate blank samples were included to verify the reliability of the method (Supplementary Information, Table S2).

2.6. HM Determination in analytical extracts

HM concentrations in the extracts from all matrices (i.e., soils and plants) were determined using inductively coupled plasma-optical emission spectrometry (ICP-OES) according to the 6010 C protocol from the USEPA (USEPA, 1997). Curve calibration solutions were prepared by diluting certified standard solutions (Multielement Standard Solution 5, TraceCERT®) to guarantee quality control in determining HMs concentrations. Analytical standards were within 10 % of known values. The analytical blanks contained Cr, Cu, Ni, and Pb concentrations below the limit of quantification (LQ) of 0.005 mg L^{-1}, and the analytical precision (expressed as RSD%) was < 10 % for all elements (Tables S1 and S2). The recovery rates of HMs (approximately 90 %) were considered satisfactory (Tables S1 and S2).

2.7. Calculations and statistical analysis

The bioconcentration factor, calculated as the ratio of concentrations in the plants and soil (BCF; (Fawzy et al., 2012)), was determined as follows (Eq. 1):

$$BCF = \frac{Metal\ content\ in\ plant\ tissue\left(\frac{mg}{kg}\right)}{Metal\ total\ content\ in\ the\ soil\left(\frac{mg}{kg}\right)} \quad (1)$$

The non-parametric Kruskal-Wallis test was applied to the data from soils and plants. If significant differences were found ($p < 0.05$), average values were compared by Dunn's post-test (Reimann et al., 2011). We applied to the data a principal component analysis with plants (e.g., Cr-shoot, Ni-shoot, Cu-root, and Pb-root) and soil parameters (HM geochemical fractions and pH of rhizosphere soil) (Reimann et al., 2011). The variables were selected to maximize the data variability within the least number of components. All statistical analyses were performed using R (Core Team, R, 2021).

3. Results

3.1. Soil bulk pH and Eh and rhizosphere pH

There were no differences between the three studied plant species concerning bulk soil pH and redox potential (Eh) (Fig. S3). On average, bulk soil pH was 5.2 ± 0.3 (Fig. S3A), whereas Eh was, on average, +242 ± 110 mV (Fig. S3B). In contrast, the pH of the rhizosphere soil under the studied plant species showed significant ($p < 0.05$) differences (Fig. 2). *T. domingensis* soil presented the most acidic rhizosphere pH (4.7 ± 0.3; Fig. 2), followed by *H. tiliaceus* (6.1 ± 0.4; Fig. 2) and *E. acutangula* (6.4 ± 0.1; Fig. 2).

3.2. Total HM contents in soils

The total HM content in the soils of the *Rio Doce* estuary (Fig. 3) varied among the different plant species. Lesser total contents of Cr, Cu, and Ni were found in the soils under the *T. domingensis* and *E. acutangula* (Cr: 13.3 ± 9 mg kg^{-1}; Cu: 12.0 ± 8.7 mg kg^{-1} and Ni: 5.0 ± 3.1 mg kg^{-1}; Fig. 3A and 3B), compared to the soils under *H. tiliaceus* (Cr: 37.6 ± 11.5 mg kg^{-1}; Cu: 31.7 ± 17.8 mg kg^{-1}, and Ni: 12.8 ± 2.9 mg kg^{-1}; Fig. 3C). The total HM contents in the soils vegetated by the macrophyte species *T. domingensis* and *E. acutangula* were not significantly different from one another; for Cr, Cu, and Ni, the average concentration for the two macrophyte species were 61–64 % lesser (Cr: 13.4 ± 8.7 mg kg^{-1}; Cu: 11.9 ± 8.7 mg kg^{-1}; Ni: 11.9 ± 8.7 mg kg^{-1}, Fig. 3) than total HMs contents in the soil vegetated by *H. tiliaceus* (Cr: 37.6 ± 11.5 mg kg^{-1}; Cu: 31.2 ± 17.7 mg kg^{-1}; Ni: 12.8 ± 2.9 mg kg^{-1}, Fig. 3). However, for Pb, the total soil content did not differ between the studied plant species (on average 71.8 ± 52.4 mg kg^{-1}; Fig. 3D).

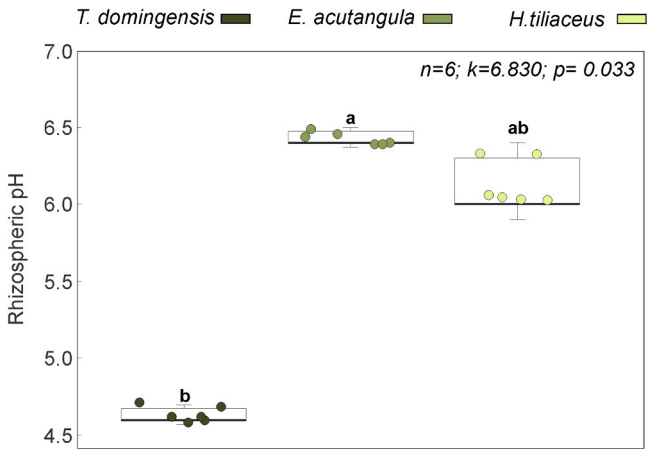

Fig. 2. Average pH values of rhizosphere soils vegetated by *T. domingensis*, *E. acutangula*, and *H. tiliaceus* at *Rio Doce* estuary (Brazil). Averages (n = 6) followed by different letters significantly differed by the Kruskal–Wallis test ($p < 0.05$).

3.3. Soil geochemical fractionation of HMs

Plant species significantly affected the geochemical fractionation of HMs in the studied soils (Fig. 4). Macrophytes (i.e., *T. domingensis* and *E. acutangula*) showed similar geochemical fractionation patterns for all HMs (Fig. 4A, 4B, 4D, 4E, 4G, 4H, 4J, and 4K). Overall, the HMs in macrophyte soils were mostly associated with short-range Fe oxides (SRO: on average 59 %), followed by crystalline Fe oxides (CO: on average 23 %), and greater percentages of BA fractions (on average 9 %) when compared to *H. tiliaceus*.

In contrast, *H. tiliaceus* soils showed significantly greater contents of HMs associated with CO (51 %) than those observed in soils vegetated by macrophytes (Cr: 1.7-fold greater; Cu: 68-fold greater; Ni: 4-fold greater; Fig. 4C, 4F, 4I, and 4L). This pattern was observed at both depths. The percentages of SRO and BA fractions were 33 % and 9 %, respectively.

3.4. HMs accumulation in plant parts and iron plaques

The pattern of HM accumulation differed between different plant parts and species (Fig. 5). For all studied species, Cr and Ni mostly accumulated in aerial tissues (i.e., shoots). Cr concentration in *T. domingensis'* shoot was 2.5-fold (178 ± 9.3 mg kg^{-1}; Fig. 5A) greater than in *E. acutangula* (72.3 ± 27.8 mg kg^{-1}; Fig. 5A), and 15-fold greater than in *H. tiliaceus* (11.5 ± 12.5 mg kg^{-1}; Fig. 5A). Similarly, Ni concentrations in *T. domingensis* (113 ± 5.1 mg kg^{-1}; Fig. 5A) were 6-fold and 9-fold greater in its shoots than *E. acutangula* (18.4 ± 5.5 mg kg^{-1}; Fig. 5A) and *H. tiliaceus* (12.3 ± 1.6 mg kg^{-1}; Fig. 5A), respectively. Conversely, Cu and Pb mostly accumulated in the roots. *H. tiliaceus* showed greater contents of Cu (58.2 ± 34.3 mg kg^{-1}; Fig. 5A) and Pb (12.7 ± 7.8 mg kg^{-1}; Fig. 5A) in its roots when compared to *E. acutangula* (Cu: 30.3 ± 27.6 mg kg^{-1}; Pb: not detected; Fig. 5A) and *T. domingensis* (Cu: 16.0 ± 12.9 mg kg^{-1}; Pb: 1.1 ± 1.4 mg kg^{-1}; Fig. 5A).

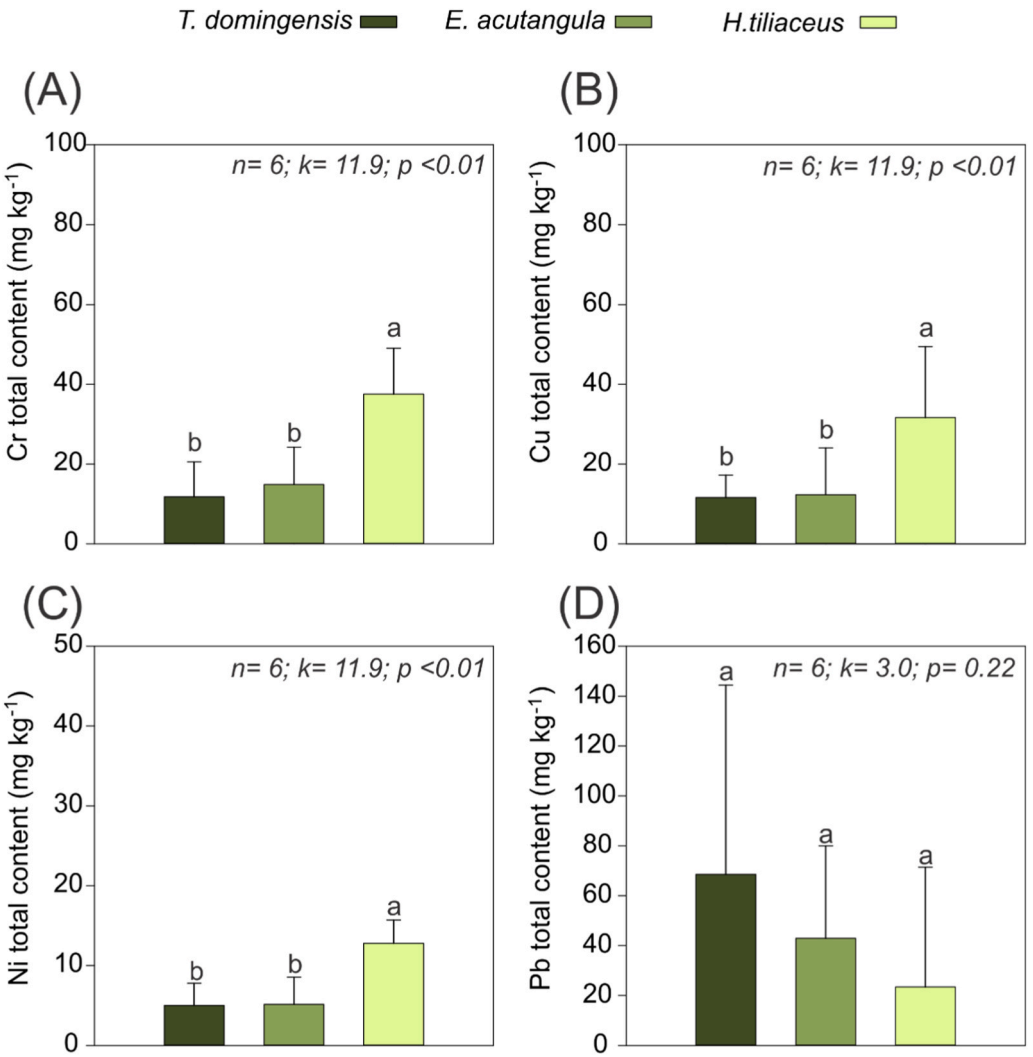

Fig. 3. Total contents of Cr (A), Cu (B), Ni (C), and Pb (D) in the soils (0–20 cm) at the *Rio Doce* estuary vegetated by *T. domingensis*, *E. acutangula,* and *H. tiliaceus*. Averages (n = 6) followed by different letters significantly differed by the Kruskal–Wallis test ($p < 0.05$).

In the iron plaques (IP) collected from roots, no significant differences were observed between the studied species for Ni and Cr, and these metals were not detected in the IP of *H. tiliaceus* and *T. domingensis* (i.e., less than the detection limit of 1.5 mg kg^{-1}; Fig. 5A). However, greater Cu concentrations were found in the *E. acutangula* (14.2 ± 8.9 mg kg^{-1}; Fig. 5A) when compared to *H. tiliaceus* (10.6 ± 10.2 mg kg^{-1}; Fig. 5A) and *T. domingensis* (1.6 ± 1.1 mg kg^{-1}; Fig. 5A). For Pb, the greatest concentration was found in *H. tiliaceus* (3.1 ± 1.6 mg kg^{-1}; Fig. 5A), followed by *T. domingensis* (1.7 ± 0.9 mg kg^{-1}; Fig. 5A) and *E. acutangula* (1.0 ± 0.6 mg kg^{-1}; Fig. 5A).

For the macrophytes, *T. domingensis* and *E. acutangula*, the shoot BCFs were > 1 for Cr (15.1 and 4.8 %, respectively), Cu (1.4 and 1.7, respectively), and Ni (22.5 and 3.6, respectively), whereas *H. tilliaceus* showed BCFs < 1 (shoot and root) for all HMs (except for Cu in roots, 2.2; Fig. 5B).

3.5. Principal component analysis

The principal component analysis (PCA) also showed clear differentiation between macrophytes (i.e., *T. domingensis* and *E. acutangula*) and *H. tilliaceus*. The two components (PC1 and PC2) obtained in the PCA explained 69.8 % of the data variability (Fig. 6; Table S3). The eigenvalues and eigenvectors of each component are presented in the Supplementary Material (see Table S3). PC1 explained 47.8 % of the data variability. In PC1, the vectors of the Cr-shoot and Ni-shoot showed opposite trends concerning Cr-SRO and pH-rhz (Fig. 6). PC2 explained 22.2 % of the data variability, and opposite directions were observed for Cr-shoot, Ni-shoot, Cr-BA, Pb-CO, Ni-Co, Ni-SRO, Ni-BA, Cr-CO, and pH-rhz (Fig. 6).

4. Discussion

The differences in HM accumulation pattern within the plants is controlled by specific biological factors that govern the transport and distribution of elements in plants (Feng et al., 2013, 2016). *T. domingensis* accumulated more Cr and Ni in the aerial tissues; however, the mechanisms involved in Cr and Ni hyperaccumulation by macrophytes (e.g., *T. domingensis*) remain poorly understood (Jaffré et al., 2013). Chromium is a non-essential element and thus lacks a specific plant transport system (Shanker et al., 2005; Sharma et al., 2020). Phosphate and sulfate transporters are plants' most common Cr uptake mechanisms (Caldelas et al., 2012; Mangabeira et al., 2011). However, in some Fe hyperaccumulators (e.g., *Brassica rapa* and *Spinacia oleracea*), Cr can be taken up and translocated by Fe channels (Cary et al., 1977), allowing its passage and accumulation (Ao et al., 2022). Additionally, some metal transporters involved in Fe and Mn accumulation in plants (e.g., NRAMP, IREG/FPN, YSL, and ZIP/IRT families) may be involved in Ni hyperaccumulation (Rascio and Navari-Izzo,

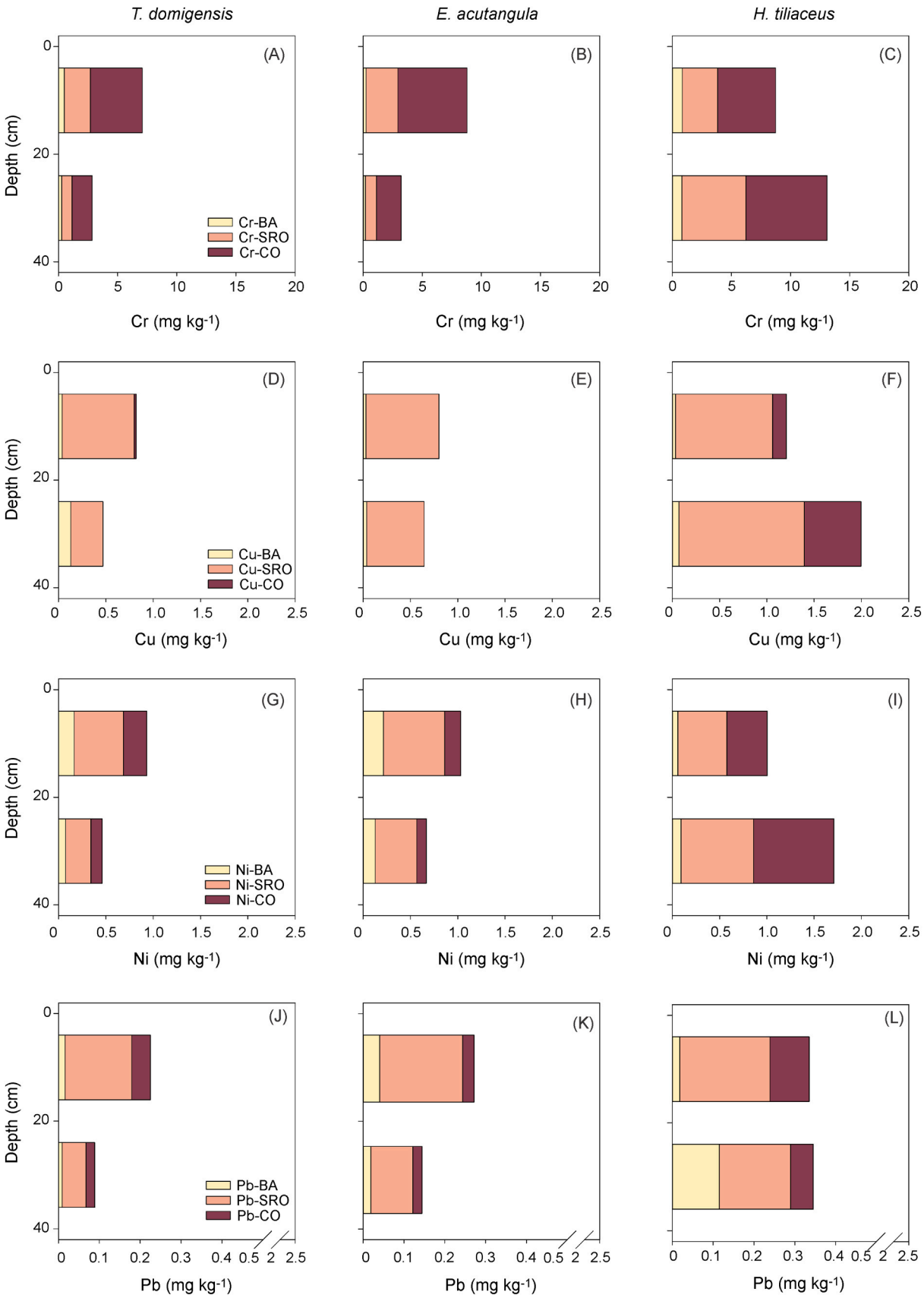

Fig. 4. Cr (A, B, and C), Cu (D, E, and F), Ni (G, H, and I), and Pb (J, K, and L) geochemical fractionation of soils under different native estuarine plant species: *T. domingensis* (A, D, G, and J), *E. acutangula* (B, E, H, and K), and *H. tiliaceus* (C, F, I and L) in the *Rio Doce* estuary. BA: bioavailable (sum of exchangeable and carbonates fractions); SRO: Short-range ordered Fe oxides (sum of ferrihydrite and lepidocrocite fractions); CO: Crystalline Fe oxides. Note: graphs A, B, and C were displayed on a different scale from the others.

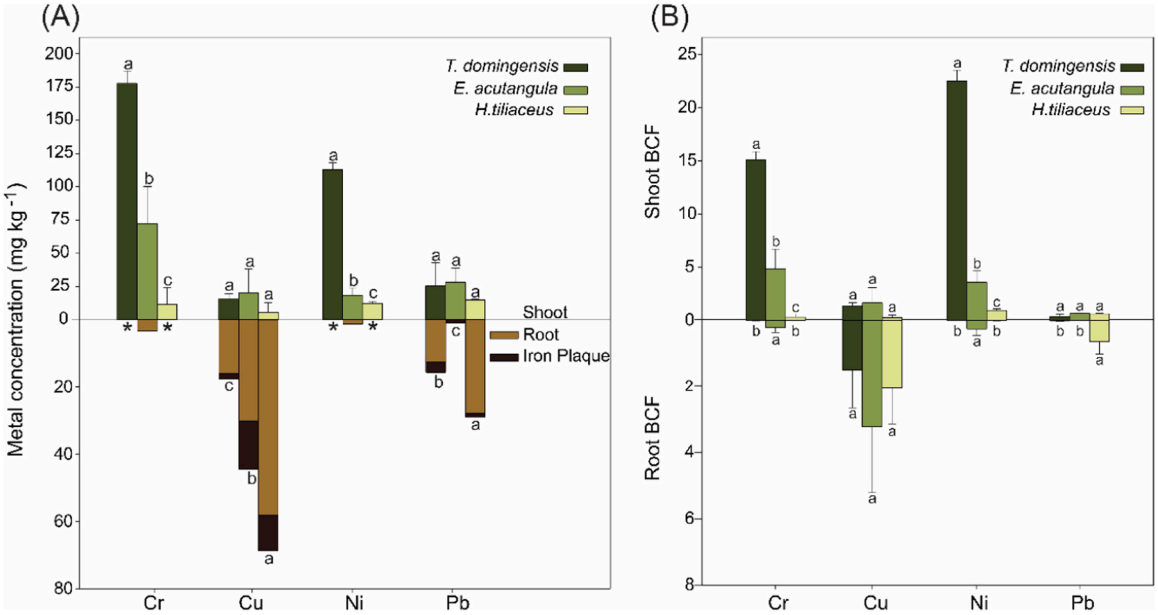

Fig. 5. Average metal concentration (mg kg^{-1}) in the iron plaque (IP), roots, and shoots of three studied estuarine plant species (*H. tiliaceus*, *E. acutangula,* and *T. domingensis*) (A) and the bioconcentration factors (BCFs) in the shoot and the root of these plants (B). Averages (n = 6) followed by different letters significantly differed by the Kruskal–Wallis test ($p < 0.05$). Statistical letters in the bottom graphs refer to the total below-ground concentration (i.e., the sum of IP and root concentrations). *Below the detection limit (1.5 mg kg^{-1}).

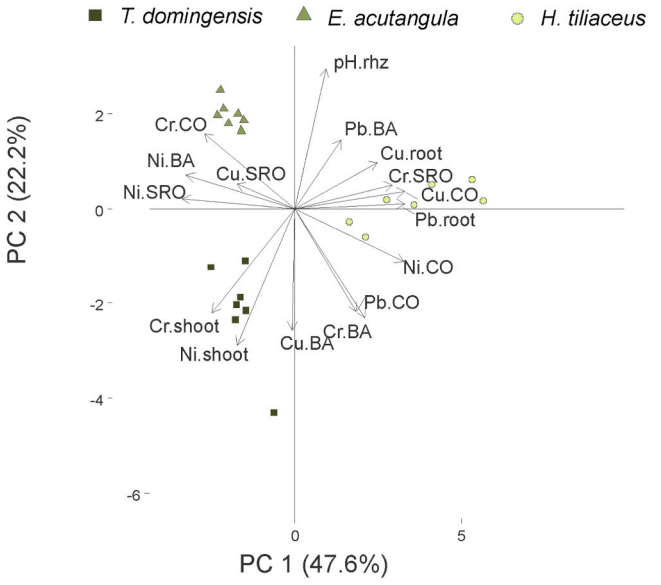

Fig. 6. Principal component analysis for soil parameters (geochemical fractions of Cr, Ni, and Cu, and rhizosphere pH (rhz-pH), and plant parameters (Cr and Ni in the shoot, Cu and Pb in the roots). All parameters were determined in the soils and plant parts of the studied plant species: *H. tiliaceus*, *E. acutangula*, and *T. domingensis*. No rotation was applied, and variables were selected to increase the data variability explained by the components.

2011; Verbruggen et al., 2009; Krämer, 2010).

Overall, the concentration of Cr and Ni in *T. domingensis* was higher than the concentration expected in plant tissues (Table 2), and within the range of concentration in the shoot of macrophytes with potential for Cr and Ni accumulation. Thus, the potential of *T. domingensis* to accumulate Cr and Ni, especially compared to the other species in this study (Fig. 5), could be associated with its ability to accumulate Fe and Mn (Ferreira et al., 2022a, 2022b; Ao et al., 2022). Non-linear logarithmic regression was adjusted. It showed a positive correlation between Cr

Table 2
Concentration of Cr, Ni, Pb and Cu in different aquatic plant species.

Plant species	Metal (range in plants*)	Concentration in the shoot	Reference
Salvinia herzogii	Cr (1.5 mg kg^{-1})	448 mg kg^{-1}	Maine et al., 2004
Typha angustata		34 mg kg^{-1}	Ramachandra et al., 2018
Phragmites australis		25.2 mg kg^{-1}	Nawrot et al., 2023
Iris pseudacorus		537 mg kg^{-1}	Nawrot et al., 2023
Callitriche cophocarpa		470 mg kg^{-1}	Augustynowicz et al., 2010
Typha angustata	Cu (10 mg kg^{-1})	165 mg kg^{-1}	Ramachandra et al., 2018
Lemna trisulca L.		550 mg kg^{-1}	Prasad et al., 2001
Potamogeton pectinatus L.		2000 mg kg^{-1}	Costa et al., 2018
Myriophyllum aquaticum		3.39	Harguinteguy et al., 2016
Potamogeton pectinatus		10.5	Baldatoni et al., 2005
Typha angustata	Ni (1.5 mg kg^{-1})	17.1 mg kg^{-1}	Ramachandra et al., 2018
Salvinia minima		163 mg kg^{-1}	Fuentes et al., 2014
Lythrum salicaria		697 mg kg^{-1}	Bingöl et al., 2017
Egeria densa		5000 mg kg^{-1}	Harguinteguy et al., 2015
Myriophyllum aquaticum		5000 mg kg^{-1}	Harguinteguy et al., 2015
Typha angustata	Pb (1 mg kg^{-1})	59.7 mg kg^{-1}	Ramachandra et al., 2018
Egeria densa		3799 mg kg^{-1}	Harguinteguy et al., 2015
Myriophyllum aquaticum		2302 mg kg^{-1}	Harguinteguy et al., 2015

*Standard reference plant concentration according to van Der Ent et al., 2013

(r^2= 0.884) and Ni (r^2= 0.883) and Fe concentrations in the shoot (Fig. 7), suggesting homology in the mechanism of accumulation. The β_1 coefficients, which represent the slope of regression lines (Cr: 62.38 and Ni: 40.57), indicated that every 1 mg kg^{-1} of Fe taken up and transported to shoots is associated with the accumulation of 0.62 mg kg^{-1} of

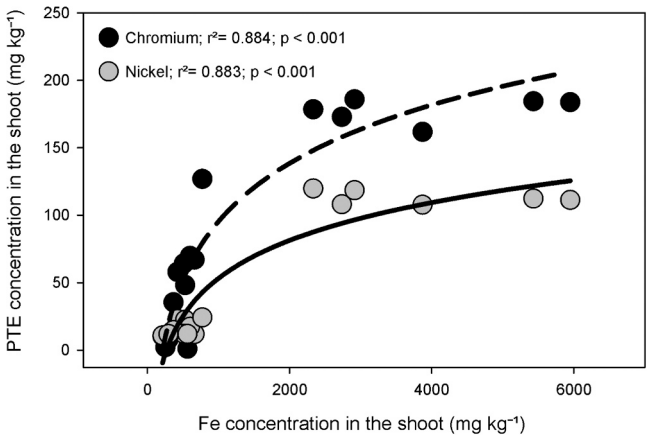

Fig. 7. Correlation between Fe, Cr, and Ni concentration in the shoots of all plant species.

Cr and 0.40 mg kg^{-1} of Ni.

In contrast, the greater accumulation of Cu and Pb in the roots of *H. tiliaceus*, followed by *E. acutangula;* Fig. 5), is probably related to the limited mobility of these elements in plants (Yan et al., 2022; Klink et al., 2013). Feng et al (Feng et al., 2016). suggested that Pb is not an essential nutrient, so it has low mobility from roots to shoots compared to critical elements (e.g., Fe). Accordingly, Cu is strongly associated with Fe in the plant roots' epidermis, implying Cu's adsorption on Fe (oxyhydr)oxides (Feng et al., 2016). The greater contents of Cu in the IP of *H. tiliaceus* and *E. acutangula* (Fig. 5A) support this interpretation. In the case of *H. tiliaceus*, BCF > 1 (for Cu and Pb roots; Fig. 5B) suggests that this species is suitable for phytostabilization programs (de Oliveira et al., 2022; Heckenroth et al., 2022).

The mobility of HMs between plant compartments may vary widely between plant species while also being influenced by intraspecific factors (Klink et al., 2013). For instance, although *Eleocharis acicularis* was reported as a Cu hyperaccumulator (accumulating up to 20,000 mg kg^{-1} of Cu in its shoots; (Sakakibara et al., 2011)), our results revealed that *Eleocharis acutangula* showed moderate HM accumulation, mainly in its roots (mostly Cu and Pb; Fig. 5A), indicating a possible species-specific mechanism of HM uptake (Yan et al., 2022; Yaashikaa et al., 2022).

On the other hand, regarding phytoextraction programs, *H. tiliaceus* and *E. acutangula* are not suitable since they showed HM concentration in the shoot higher than expected for a plant, but much lower than the hyperaccumulation threshold (Van der Ent et al., 2013) and the range of concentration in potential phytoextractor species (Table 2).

Interactions between biological and geochemical conditions can explain the patterns of HM in the studied soils (Fig. 4) and HM accumulation in the plant parts (Fig. 5). The lesser total HM content in the soils vegetated by macrophytes (i.e., *Typha* and *E. acutangula*. Fig. 3) exemplifies the contrasting potential of estuarine plant species to alter soil geochemistry (Ferreira et al., 2022a; Manasypov et al., 2021), which ultimately leads to differences in the dynamics of HMs in soils (Fig. 4; (Ao et al., 2022)). Understanding how plants control the soil biogeochemistry of HMs may elucidate the factors influencing the bioavailability of metals in soils colonized by different plant species (Ferreira et al., 2022a, 2022b).

The contrasting rhizosphere soil conditions (e.g., pH; Fig. 2) observed for each plant species exerted major control over HM biogeochemistry and affected plant HMs accumulation potential. Among the studied plants, *T. domingensis* showed the most acidic rhizosphere pH (Fig. 2) and the greatest Cr and Ni contents in its shoots (Fig. 5A). This relationship was expressed by the opposite vectors between rhz-pH and Ni-BA and Ni-SRO in PC1 and the opposite vectors between rhz-pH and Ni-shoot in PC2 (Fig. 6; Table S3). The lesser Ni content associated with SRO and BA, especially in Typha soils (Fig. 4G), is probably related to the dissolution of SRO fraction, which is more prone to dissolution at acidic pH (Miller et al., 1986; Schwertmann, 1991). The dissolution process can concomitantly release HMs associated with SRO Fe minerals (see (Queiroz et al., 2021)), which plants can then take up, resulting in greater Cr and Ni absorption. This interpretation is corroborated by the high concentration of Cr and Ni in Typha shoots (Fig. 5A). In fact, rhizosphere pH has been well-reported as a parameter that has a significant effect on the metal acquisition by different hyperaccumulator plants (Alejandro et al., 2020; DeGroote et al., 2018).

In contrast, the soils vegetated with *H. tiliaceus* and *E. acutangula* showed HMs mostly associated with iron oxides (Fig. 4B, 4C, 4E, 4F, 4H, 4I, 4K, and 4L). The profuse and well-distributed root systems of both plants are highly efficient in promoting bioturbation (i.e., disturbance of soil and sediment layers by biological activity; (Kristensen et al., 2012)), which increases soil porosity (Martínez-Sánchez et al., 2022), favors oxygen diffusion into the soil (Machado et al., 2014), and leads to Fe oxide precipitation (Mendelssohn and Postek, 1982).

Additionally, rhizosphere pH affected HM accumulation in *H. tiliaceus* and *E. acutangula* roots. For instance, the large magnitude of eigenvalues and the same direction of eigenvectors for rhz-pH and SRO in PC2 (Fig. 6; Table S3) indicated a positive correlation between these variables. Thus, a more alkaline rhizosphere pH would favor SRO precipitation and HM adsorption with this fraction (Fig. 4F). In fact, Moon and Peacock (Moon and Peacock, 2013) demonstrated that increased pH increased favored Cu adsorbed by inner-sphere complexes on SRO surfaces. Bravin et al (Bravin et al., 2009). showed that soil alkalinization by roots is an important plant strategy for coping with Cu^{2+} phytotoxicity. These authors observed a decrease in Cu^{2+} activity of up to three orders of magnitude with increasing pH in the *Triticum turgidum durum* L. rhizosphere. Various studies (de Oliveira et al., 2022; Bravin et al., 2009) have shown that root accumulation is an important mechanism controlling Cu content. These findings were further corroborated by Cu root content in *H. tiliaceus* and *E. acutangula* (Fig. 5).

In this sense, HM total contents can widely vary between bulk and rhizosphere soil due to the biogeochemical changes induced by plants (Wang et al., 2002; Wang et al., 2023), which also impacts the elements uptake by plants (Wiche and Pourret, 2023). The pH of the rhizosphere is a key factor in determining the bioavailability of HM in soils. Higher pH levels in the rhizosphere tend to decrease heavy metal bioavailability (Bravin et al., 2009), while lower pH levels can increase it (Alejandro et al., 2020; DeGroote et al., 2018).

It is also important to note that HM bioavailability (Fig. 4) may not result in increased HM uptake (Fig. 5), as shown in *H. tiliaceus* and *E. acutangula*. These soils associated with these plants showed the greatest BA and SRO contents (Fig. 4) and the smallest HM shoot concentrations (Fig. 5A). As mentioned previously, the lack of metal transporters and non-essentiality are biological factors that may impair HM uptake and translocation (Feng et al., 2013, 2016).

HM translocation from root to shoot can provide not only guidelines for phytoremediation protocols (i.e., phytoextraction or phytostabilization) but also shed light on potential environmental risks of each HM based on the plant compartments in which they accumulate. For instance, HMs accumulated in the roots would not be accessed by herbivores, possibly decreasing the environmental risks of animals consuming contaminated plant compartments (Jackson, 1998). On the other hand, fast root decay can cycle the HMs in the environment. HM accumulation in leaves can facilitate the removal of contaminants from the environment in cases where plant management is applied; however, if the aerial tissues are not harvested, leaf senescence and shoot transport by rivers could export HMs to other environments (Jackson, 1998). Besides the importance of metals global cycling, there is a lack of information in how different accumulation patterns between aquatic plants (i.e., root, stem, or leaves) could impact the heavy metals fates.

5. Conclusions

Our study sheds light on new pathways toward plant control of heavy metals (HM) dynamics in estuarine soils and its implications for potential phytoremediation strategies targeting HM decontamination. Our findings show contrasting potentials for HM phytoremediation by different tropical native estuarine plants. Cr and Ni accumulated the most in the shoots of naturally growing *T. domingensis*. In contrast, *H. tiliaceus* accumulated more Cu and Pb in the roots, indicating great potential for the phytostabilization of these hazardous elements. To our knowledge, this is the first report of *H. tiliaceus* as a suitable species for Cu and Pb phytostabilization in wetland environments. The contrasting soil rhizosphere pH among plant species significantly influenced the dynamics of HMs in soils, affecting Fe (oxyhydr)oxide dissolution and precipitation, which controlled HM accumulation in plant parts.

Based on our findings, we highlight the potential of *T. domingensis* for the phytoextraction of multiple hazardous elements, with the potential to help mitigate the environmental impacts of Cr and Ni soil contamination. The phytoremediation potential of *Typha* could be increased through assisted phytoremediation approaches (e.g., chelated- and microbially assisted phytoextraction (Sarwar et al., 2017)). Finally, *E. acutangula* showed the least potential for HM phytoremediation.

CRediT authorship contribution statement

Hermano Melo Queiroz: Writing – review & editing, Validation, Methodology, Formal analysis. **Amanda Duim Ferreira:** Writing – review & editing, Writing – original draft, Methodology, Formal analysis, Data curation, Conceptualization. **Owen W. Duckworth:** Writing – review & editing, Supervision, Project administration, Funding acquisition. **Alexys Giorgia Friol Boim:** Writing – review & editing, Data curation. **Angelo Fraga Bernardino:** Writing – review & editing, Project administration, Investigation. **Xosé L. Otero:** Writing – review & editing, Investigation, Funding acquisition. **Tiago Osório Ferreira:** Writing – review & editing, Supervision, Project administration, Investigation, Funding acquisition, Conceptualization.

Declaration of Competing Interest

The authors declare that they have no known competing financial interests or personal relationships that could have appeared to influence the work reported in this paper.

Data availability

Data will be made available on request.

Acknowledgements

We thank the "Luiz de Queiroz" Agricultural Studies Foundation (FEALQ). This work was also supported by Fundação de Amparo do Espírito Santo (FAPES/CNPq/CAPES Rio Doce 77683544/2017); Coordenação de Aperfeiçoamento de Pessoal de Nível Superior CAPES—Finance Code 001 and CNPq (grant numbers, AFB: 301161/2017-8, TOF: 305996/2018-5); and the São Paulo Research Foundation (FAPESP, ADF grant number 2019/14800-5 and 2022/00296-6; HMQ grant number 2018/04259-2 and 2021/00221-3; TOF grant numbers 2019/19987-6 and 2018/08408-2; AGFB: 2020/12823-5). XLO was supported by Xunta de Galicia-Consellería de Educación e Ordeanción Universitaria de Galicia (Consolidation of competitive groups of investigation; GRC GI 1574) and the CRETUS strategic group (AGRUP2015/02). OWD was supported by National Institute of Food and Agriculture (USDA Hatch project NC02713).

Appendix A. Supporting information

Supplementary data associated with this article can be found in the online version at doi:10.1016/j.ecoenv.2024.116416.

References

Alejandro, S., Höller, S., Meier, B., Peiter, E., 2020. Manganese in plants: from acquisition to subcellular allocation. Front. Plant Sci. 11, 300. https://doi.org/10.3389/FPLS.2020.00300/BIBTEX.

Ao, M., Chen, X., Deng, T., Sun, S., Tang, Y., Morel, J.L., Qiu, R., Wang, S., 2022. Chromium biogeochemical behaviour in soil-plant systems and remediation strategies: a critical review. J. Hazard Mater. 424, 127233 https://doi.org/10.1016/J.JHAZMAT.2021.127233.

Augustynowicz, Joanna, Marek Grosicki, Ewa Hanus-Fajerska, Małgorzata Lekka, Andrzej Waloszek, Henryk, Kołoczek, 2010. Chromium (VI) bioremediation by aquatic macrophyte Callitriche cophocarpa Sendtn. Chemosphere 79 (11), 1077–1083.

Baksh, S.I., 2006. An architectural model for Eleocharis: morphology and development of Eleocharis cellulosa (Cyperaceae)Am. J. Bot. 93, 707–715. https://doi.org/10.3732/AJB.93.5.707.

Baldantoni, D., Maisto, G., Bartoli, G., Alfani, A., 2005. Analyses of three native aquatic plant species to assess spatial gradients of lake trace element contamination. Aquatic botany 83 (1), 48–60.

Barcellos, D., Queiroz, H.M., Ferreira, A.D., Bernardino, A.F., Nóbrega, G.N., Otero, X.L., Ferreira, T.O., 2022. Short-term Fe reduction and metal dynamics in estuarine soils impacted by Fe-rich mine tailings. Appl. Geochem. 136, 105134 https://doi.org/10.1016/J.APGEOCHEM.2021.105134.

Bernardino, A.F., Netto, S.A., Pagliosa, P.R., Barros, F., Christofoletti, R.A., Rosa Filho, J. S., Colling, A., Lana, P.C., 2015. Predicting ecological changes on benthic estuarine assemblages through decadal climate trends along Brazilian Marine Ecoregions. Estuar. Coast Shelf Sci. 166, 74–82. https://doi.org/10.1016/J.ECSS.2015.05.021.

Bernardino, A.F., Pais, F.S., Oliveira, L.S., Gabriel, F.A., Ferreira, T.O., Queiroz, H.M., Mazzuco, A.C.A., 2019. Chronic trace metals effects of mine tailings on estuarine assemblages revealed by environmental DNA. PeerJ 2019, e8042. https://doi.org/10.7717/PEERJ.8042/SUPP-6.

Bingöl, N.A., Özmal, F., Akın, B., 2017. Phytoremediation and biosorption potential of lythrum salicaria l. for nickel removal from aqueous solutions. Polish Journal of Environmental Studies 26 (6), 2479–2485.

Bissoli, L.B., Bernardino, A.F., 2018. Benthic macrofaunal structure and secondary production in tropical estuaries on the Eastern Marine Ecoregion of Brazil. PeerJ 2018, e4441. https://doi.org/10.7717/PEERJ.4441/SUPP-2.

Bravin, M.N., Tentscher, P., Rose, J., Hinsinger, P., 2009. Rhizosphere pH gradient controls copper availability in a strongly acidic soil. Environ. Sci. Technol. 43, 5686–5691. https://doi.org/10.1021/ES900055K/SUPPL_FILE/ES900055K_SI_001.PDF.

Caldelas, C., Bort, J., Febrero, A., 2012. Ultrastructure and subcellular distribution of Cr in Iris pseudacorus L. using TEM and X-ray microanalysis. Cell Biol. Toxicol. 28, 57–68.

Cary, E.E., Allaway, W.H., Olson, O.E., 1977. Control of chromium concentrations in food plants. 1. Absorption and translocation of chromium by plants. J. Agric. Food Chem. 25, 300–304.

R. Core Team, R, (2021). http://www.r-project.org/index.html (accessed December 28, 2020).

Costa, Marcela Brandão, Francesca Valêncio Tavares, Claudia Bueno Martinez, Ioni Gonçalves Colares, and Camila de Martinez Gaspar Martins. Accumulation and effects of copper on aquatic macrophytes Potamogeton pectinatus L.: Potential application to environmental monitoring and phytoremediation. *Ecotoxicology and Environmental Safety* 155 (2018): 117-124.

D.J. Rosen, S.L. Hatch, R. CarterInfraspecific taxonomy and nomenclature of ELEOCHARIS acutangula (cyperaceae)J. Bot. Res. Inst. Tex., 1 (2007), pp. 875-888.

De Luca Rebello, A., Haekel, W., Moreira, J., Santelli, R., Schroeder, F., 1986. The fate of heavy metals in an estuarine tropical system. Mar. Chem. 18, 215–225. https://doi.org/10.1016/0304-4203(86)90009-5.

de Oliveira, D.P., Queiroz, H.M., Perlatti, F., Ferreira, A.D., Asensio, V., Nóbrega, G.N., Otero, X.L., Ferreira, T.O., 2022. Cu dynamics in the rhizosphere of native tropical species: assessing the potential for phytostabilization in mining-impacted soils. Minerals 2022 Vol. 12 (12), 130, 130. https://doi.org/10.3390/MIN12020130.

DeGroote, K.V., McCartha, G.L., Pollard, A.J., 2018. Interactions of the manganese hyperaccumulator Phytolacca americana L. with soil pH and phosphate. Ecol. Res. 33, 749–755. https://doi.org/10.1007/S11284-017-1547-Z.

Edwards, J., Johnson, C., Santos-Medellín, C., Lurie, E., Podishetty, N.K., Bhatnagar, S., Eisen, J.A., Sundaresan, V., Jeffery, L.D., 2015. Structure, variation, and assembly of the root-associated microbiomes of rice. Proc. Natl. Acad. Sci. USA 112, E911–E920. https://doi.org/10.1073/pnas.1414592112.

Enya, O., Lin, C., Qin, J., 2019. Heavy metal contamination status in the soil-plant system in the Upper Mersey Estuarine Floodplain, Northwest England. Mar. Pollut. Bull. 146, 292–304. https://doi.org/10.1016/J.MARPOLBUL.2019.06.026.

Fadzil, F.N.M., Mohamad, M.A.N., Repin, R., Harumain, Z.A.S., 2023. Metal uptake and tolerance in hyperaccumulator plants: Advancing phytomining strategies. *Rhizosphere*, p. 100836.

Fawzy, M.A., Badr, N.E., El-Khatib, A., Abo-El-Kassem, A., 2012. Heavy metal biomonitoring and phytoremediation potentialities of aquatic macrophytes in River

Nile. Environ. Monit. Assess. 184, 1753–1771. https://doi.org/10.1007/s10661-011-2076-9.
Feng, H., Qian, Y., Gallagher, F.J., Wu, M., Zhang, W., Yu, L., Zhu, Q., Zhang, K., Liu, C.-J., Tappero, R., 2013. Lead accumulation and association with Fe on Typha latifolia root from an urban brownfield site. Environ. Sci. Pollut. Res. 20, 3743–3750.
Feng, H., Qian, Y., Gallagher, F.J., Zhang, W., Yu, L., Liu, C., Jones, K.W., Tappero, R., 2016. Synchrotron micro-scale measurement of metal distributions in Phragmites australis and Typha latifolia root tissue from an urban brownfield site. J. Environ. Sci. 41, 172–182.
Ferreira, T.O., Otero, X.L., Vidal-Torrado, P., Macías, F., 2007. Effects of bioturbation by root and crab activity on iron and sulfur biogeochemistry in mangrove substrate. Geoderma 142, 36–46. https://doi.org/10.1016/J.GEODERMA.2007.07.010.
Ferreira, A.D., Queiroz, H.M., Barcellos, D., Otero, X.L., Nóbrega, G.N., Bernardino, Â.F., Ferreira, T.O., 2022b. Screening for natural manganese scavengers: Divergent phytoremediation potentials of wetland plants. J. Clean. Prod. 365, 132811 https://doi.org/10.1016/J.JCLEPRO.2022.132811.
Ferreira, A.D., Queiroz, H.M., Otero, X.L., Barcellos, D., Bernardino, Â.F., Ferreira, T.O., 2022a. Iron hazard in an impacted estuary: contrasting controls of plants and implications to phytoremediation. J. Hazard Mater. 428, 128216 https://doi.org/10.1016/J.JHAZMAT.2022.128216.
Fuentes, I.I., Espadas-Gil, F., Talavera-May, C., Fuentes, G., Santamaría, J.M., 2014. Capacity of the aquatic fern (Salvinia minima Baker) to accumulate high concentrations of nickel in its tissues, and its effect on plant physiological processes. Aquatic Toxicology 155, 142–150.
Gabriel, F., Hauser-Davis, R.A., Soares, L., Mazzuco, A.C.A., Rocha, R.C.Chavez, Saint Pierre, T.D., Saggioro, E., Correia, F.V., Ferreira, T.O., Bernardino, A.F., 2020b. Contamination and oxidative stress biomarkers in estuarine fish following a mine tailing disaster. PeerJ 8. https://doi.org/10.7717/PEERJ.10266.
Gabriel, F.A., Silva, A.G., Queiroz, H.M., Ferreira, T.O., Hauser-Davis, R.A., Bernardino, A.F., 2020a. Ecological risks of metal and metalloid contamination in the Rio Doce estuary. Integr. Environ. Assess. Manag 16, 655–660. https://doi.org/10.1002/IEAM.4250.
G.W. Gee, J.W. Bauder, Particle-size Analysis, Methods of Soil Analysis, Part 1: Physical and Mineralogical Methods. (1986) 383–411. https://doi.org/10.2136/SSSABOOKSER5.1.2ED.C15.
Gomes, LEO, Correa, LB, Sá, F, Neto, RR, Bernardino, AF, 2017. The impacts of the Samarco mine tailing spill on the Rio Doce estuary, Eastern Brazil. Mar Pollut Bull 120 (1–2), 28–36. https://doi.org/10.1016/j.marpolbul.2017.04.056.
Hadlich, H.L., Venturini, N., Martins, C.C., Hatje, V., Tinelli, P., Gomes, L.E. de O., Bernardino, A.F., 2018. Multiple biogeochemical indicators of environmental quality in tropical estuaries reveal contrasting conservation opportunities. Ecol. Indic. 95, 21–31. https://doi.org/10.1016/j.ecolind.2018.07.027.
Harguinteguy, C.A., Cofré, M.N., Fernández-Cirelli, A., Pignata, M.L., 2016. The macrophytes Potamogeton pusillus L. and Myriophyllum aquaticum (Vell.) Verdc. as potential bioindicators of a river contaminated by heavy metals. Microchemical Journal 124, 228–234.
Harguinteguy, C.A., Pignata, M.L., Fernández-Cirelli, A., 2015. Nickel, lead and zinc accumulation and performance in relation to their use in phytoremediation of macrophytes Myriophyllum aquaticum and Egeria densa. Ecological engineering 82, 512–516.
Hatje, V., Pedreira, R.M.A., de Rezende, C.E., Schettini, C.A.F., de Souza, G.C., Marin, D. C., Hackspacher, P.C., 2017. The environmental impacts of one of the largest tailing dam failures worldwide. Sci. Rep. 7, 10706 https://doi.org/10.1038/s41598-017-11143-x.
Health, E.G., Zandi, P., Yang, J., Darma, A., Bloem, E., Xia, X., Wang, Y., Li, Q., Schnug, Ewald, Zandi, P., Yang, J., Darma, A., Xia, X., Wang, Y., Darma, A., Bloem, E., Li, Q., Schnug, E., 2022. Iron plaque formation, characteristics, and its role as a barrier and facilitator to heavy metal uptake in hydrophyte rice (Oryza sativa L.). Environ. Geochem. Health 1–35. https://doi.org/10.1007/S10653-022-01246-4.
Heckenroth, A., Prudent, P., Folzer, H., Rabier, J., Criquet, S., Saatkamp, A., Salducci, M. D., Vassalo, L., Laffont-Schwob, I., 2022. Coronilla juncea, a native candidate for phytostabilization of potentially toxic elements and restoration of Mediterranean soils. Sci. Rep. 2022 12, 1–14. https://doi.org/10.1038/s41598-022-14139-4.
J. Howard, S. Hoyt, K. Isensee, M. Telszewski, E. Pidgeon, Coastal blue carbon: methods for assessing carbon stocks and emissions factors in mangroves, tidal salt marshes, and seagrasses, 1st ed., International Union for Conservation of Nature, Arlington, VA, USA, 2014. https://cgspace.cgiar.org/handle/10568/95127 (accessed December 24, 2022).
Jackson, L.J., 1998. Paradigms of metal accumulation in rooted aquatic vascular plants. Science of the Total Environment 219 (2–3), 223–231.
Jaffré, T., Pillon, Y., Thomine, S., Merlot, S., 2013. The metal hyperaccumulators from New Caledonia can broaden our understanding of nickel accumulation in plants. Front Plant Sci. 4, 279. https://doi.org/10.3389/FPLS.2013.00279/ABSTRACT.
Jiang, H.-H., Cai, L.-M., Wen, H.-H., Hu, G.-C., Chen, L.-G., Luo, J., 2020. An integrated approach to quantifying ecological and human health risks from different sources of soil heavy metals. Sci. Total Environ. 701, 134466 https://doi.org/10.1016/j.scitotenv.2019.134466.
Klink, A., Macioł, A., Wisłocka, M., Krawczyk, J., 2013. Metal accumulation and distribution in the organs of Typha latifolia L. (cattail) and their potential use in bioindication. Limnologica 43, 164–168. https://doi.org/10.1016/J.LIMNO.2012.08.012.
Krämer, U., 2010. Metal hyperaccumulation in plants. Annu. Rev. Plant Biol. 61, 517–534.
Kristensen, E., Penha-Lopes, G., Delefosse, M., Valdemarsen, T., Quintana, C.O., Banta, G. T., 2012. What is bioturbation? The need for a precise definition for fauna in aquatic sciences. Mar. Ecol. Prog. Ser. 446, 285–302. https://doi.org/10.3354/MEPS09506.
Li, Y., Feng, W., Chi, H., Huang, Y., Ruan, D., Chao, Y., Qiu, R., Wang, S., 2019. Could the rhizoplane biofilm of wetland plants lead to rhizospheric heavy metal precipitation and iron-sulfur cycle termination? J. Soils Sediment. 19, 3760–3772. https://doi.org/10.1007/s11368-019-02343-1.
Machado, W., Borrelli, N.L., Ferreira, T.O., Marques, A.G.B., Osterrieth, M., Guizan, C., 2014. Trace metal pyritization variability in response to mangrove soil aerobic and anaerobic oxidation processes. Mar. Pollut. Bull. 79, 365–370. https://doi.org/10.1016/J.MARPOLBUL.2013.11.016.
Maine, María A., Noemí L. Suñé, and Susana C. Lagger. "Chromium bioaccumulation: comparison of the capacity of two floating aquatic macrophytes." *Water Research* 38, no. 6 (2004): 1494-1501.
Manasypov, R.M., Pokrovsky, O.S., Shirokova, L.S., Auda, Y., Zinner, N.S., Vorobyev, S. N., Kirpotin, S.N., 2021. Biogeochemistry of macrophytes, sediments and porewaters in thermokarst lakes of permafrost peatlands, western Siberia. Sci. Total Environ. 763, 144201 https://doi.org/10.1016/J.SCITOTENV.2020.144201.
Mangabeira, P.A., Ferreira, A.S., de Almeida, A.-A.F., Fernandes, V.F., Lucena, E., Souza, V.L., dos Santos Júnior, A.J., Oliveira, A.H., Grenier-Loustalot, M.F., Barbier, F., 2011. Compartmentalization and ultrastructural alterations induced by chromium in aquatic macrophytes. Biometals 24, 1017–1026.
Martínez-Sánchez, M.J., Pérez-Sirvent, C., Martínez-Lopez, S., García-Lorenzo, M.L., Agudo, I., Martínez-Martínez, L.B., Hernández-Pérez, C., Bech, J., 2022. Uptake of potentially toxic elements by edible plants in experimental mining Technosols: preliminary assessment. Environ. Geochem Health 44, 1649–1665. https://doi.org/10.1007/S10653-021-01091-X/FIGURES/7.
Mendelssohn, I.A., Postek, M.T., 1982. Elemental analysis of deposits on the roots of Spartina alterniflora Loisel. Am. J. Bot. 69, 904–912.
Miller, W.P., Zelazny, L.W., Martens, D.C., 1986. Dissolution of synthetic crystalline and noncrystalline iron oxides by organic acids. Geoderma 37, 1–13. https://doi.org/10.1016/0016-7061(86)90039-X.
Moon, E.M., Peacock, C.L., 2013. Modelling Cu(II) adsorption to ferrihydrite and ferrihydrite–bacteria composites: deviation from additive adsorption in the composite sorption system. Geochim. Cosmochim. Acta 104, 148–164. https://doi.org/10.1016/J.GCA.2012.11.030.
Nawrot, Nicole, Ewa Wojciechowska, Muhammad Mohsin, Suvi Kuittinen, Ari Pappinen, Matej-Łukowicz, Karolina, Katarzyna Szczepańska, Agnieszka Cichowska, Muhammad Atif Irshad, Filip, MG Tack, 2023. Chromium (III) removal by perennial emerging macrophytes in floating treatment wetlands. Scientific Reports 13 (1), 22417.
Otero, X.L., Ferreira, T.O., Huerta-Díaz, M.A., Partiti, C.S.M., Souza, V., Vidal-Torrado, P., Macías, F., 2009. Geochemistry of iron and manganese in soils and sediments of a mangrove system, Island of Pai Matos (Cananeia — SP, Brazil). Geoderma 148, 318–335. https://doi.org/10.1016/J.GEODERMA.2008.10.016.
Prasad, M.N.V., Przemysław Malec, Waloszek, Andrzej, Monika Bojko, Kazimierz, Strzałka., 2001. Physiological responses of Lemna trisulca L.(duckweed) to cadmium and copper bioaccumulation. Plant Science 161 (5), 881–889.
Queiroz, H.M., Ferreira, A.D., Ruiz, F., Bovi, R.C., Deng, Y., de Souza Júnior, V.S., Otero, X.L., Bernardino, A.F., Cooper, M., Ferreira, T.O., 2022. Early pedogenesis of anthropogenic soils produced by the world's largest mining disaster, the "Fundão" dam collapse, in southeast Brazil. Catena (Amst.) 219, 106625. https://doi.org/10.1016/J.CATENA.2022.106625.
Queiroz, H.M., Nóbrega, G.N., Ferreira, T.O., Almeida, L.S., Romero, T.B., Santaella, S.T., Bernardino, A.F., Otero, X.L., 2018. The Samarco mine tailing disaster: a possible time-bomb for heavy metals contamination? Sci. Total Environ. 637–638, 498–506. https://doi.org/10.1016/J.SCITOTENV.2018.04.370.
Queiroz, H.M., Ying, S.C., Bernardino, A.F., Barcellos, D., Nóbrega, G.N., Otero, X.L., Ferreira, T.O., 2021. Role of Fe dynamic in the release of metals at Rio Doce estuary: Unfolding of a mining disaster. Mar. Pollut. Bull. 166, 112267 https://doi.org/10.1016/J.MARPOLBUL.2021.112267.
Ramachandra, T.V., Sudarshan, P.B., Mahesh, M.K., 2018. Spatial patterns of heavy metal accumulation in sediments and macrophytes of Bellandur wetland, Bangalore. Journal of environmental management 206, 1204–1210.
Rascio, N., Navari-Izzo, F., 2011. Heavy metal hyperaccumulating plants: How and why do they do it? And what makes them so interesting? Plant Sci. 180, 169–181. https://doi.org/10.1016/J.PLANTSCI.2010.08.016.
C. Reimann, P. Filzmoser, R. Garrett, R. Dutter, Statistical data analysis explained: applied environmental statistics with R, John Wiley & Sons, 2011.
Sakakibara, M., Ohmori, Y., Ha, N.T.H., Sano, S., Sera, K., 2011. Phytoremediation of heavy metal-contaminated water and sediment by Eleocharis acicularis. Clean (Weinh.) 39, 735–741. https://doi.org/10.1002/CLEN.201000488.
Sarwar, N., Imran, M., Shaheen, M.R., Ishaque, W., Kamran, M.A., Matloob, A., Rehim, A., Hussain, S., 2017. Phytoremediation strategies for soils contaminated with heavy metals: modifications and future perspectives. Chemosphere 171, 710–721.
Schück, M., Greger, M., 2020a. Plant traits related to the heavy metal removal capacities of wetland plants. Int. J. Phytoremediat. 22, 427–435. https://doi.org/10.1080/15226514.2019.1669529/SUPPL_FILE/BIJP_A_1669529_SM9742.DOCX.
Schück, M., Greger, M., 2020b. Screening the capacity of 34 wetland plant species to remove heavy metals from water. Int. J. Environ. Res. Public Health Vol. 17 (17), 4623, 4623. https://doi.org/10.3390/IJERPH17134623.
Schwertmann, U., 1991. Solubility and dissolution of iron oxides. Plant Soil 130, 1–25. https://doi.org/10.1007/BF00011851/METRICS.
Shanker, A.K., Cervantes, C., Loza-Tavera, H., Avudainayagam, S., 2005. Chromium toxicity in plants. Environ. Int. 31, 739–753.

Sharma, A., Kapoor, D., Wang, J., Shahzad, B., Kumar, V., Bali, A.S., Jasrotia, S., Zheng, B., Yuan, H., Yan, D., 2020. Chromium bioaccumulation and its impacts on plants: an overview. Plants 2020 Vol. 9 (9), 100. https://doi.org/10.3390/PLANTS9010100.

Taylor, G.J., Crowder, A.A., 1983. Use of the DCB technique for extraction of hydrous iron oxides from roots of wetland plants. Am. J. Bot. 70, 1254–1257.

United States Environmental Protection Agency, Method 3052: Microwave assisted acid digestion of siliceous and organically based matrices., (1996).

USEPA, Method 6010C inductively coupled plasma-atomic emission spectometry, 2 (1997) 1–19. https://www.epa.gov/sites/production/files/2015-07/documents/epa-6010c.pdf (accessed May 3, 2018).

USEPA, 2007. Method 3051: Microwave assisted acid digestion of sediments, sludges, soils, and oils. Test Methods for Evaluating Solid Waste 1–30. https://doi.org/10.1017/CBO9781107415324.004.

Van der Ent, Antony, Alan JM Baker, Roger D. Reeves, A. Joseph Pollard, and Henk Schat. Hyperaccumulators of metal and metalloid trace elements: facts and fiction. *Plant and soil* 362 (2013): 319-334.

Varzim, C.S., Hadlich, H.L., Andrades, R., Mazzuco, A.C. de A., Bernardino, A.F., 2019. Tracing pollution in estuarine benthic organisms and its impacts on food webs of the Vitoria Bay estuary. Estuar. Coast Shelf Sci. 229, 106410 https://doi.org/10.1016/j.ecss.2019.106410.

Verbruggen, N., Hermans, C., Schat, H., 2009. Molecular mechanisms of metal hyperaccumulation in plants. New Phytol. 181, 759–776.

Verdcourt, Bernard., 2009. Geoffrey.MwachalaFlora of Tropical East Africa(first ed.), Royal Botanic Gardens. Kew.

Wang, Z., Shan, X.Q., Zhang, S., 2002. Comparison between fractionation and bioavailability of trace elements in rhizosphere and bulk soils. Chemosphere 46 (8), 1163–1171.

Wang, Q., Wei, S., Zhou, Y., Mašek, O., Khan, M.A., Li, D., Huang, Q., 2023. Rhizosphere effect on the relationship between dissolved organic matter and functional genes in contaminated soil. Journal of Environmental Management 342, 118118.

Wiche, O., Pourret, O., 2023. The role of root carboxylate release on rare earth element (hyper)accumulation in plants – a biogeochemical perspective on rhizosphere chemistry. Plant Soil 492, 79–90.

Xue, S., He, X., Jiang, X., Pan, W., Li, W., Xia, L., Wu, C., 2022. Arsenic biotransformation genes and As transportation in the soil-rice system affected by iron-oxidizing strain (Ochrobactrum sp. Environ. Pollut. 314, 120311 https://doi.org/10.1016/J.ENVPOL.2022.120311.

Yaashikaa, P.R., Kumar, P.S., Jeevanantham, S., Saravanan, R., 2022. A review on bioremediation approach for heavy metal detoxification and accumulation in plants. Environ. Pollut. 301, 119035 https://doi.org/10.1016/J.ENVPOL.2022.119035.

Yan, X., An, J., Yin, Y., Gao, C., Wang, B., Wei, S., 2022. Heavy metals uptake and translocation of typical wetland plants and their ecological effects on the coastal soil of a contaminated bay in Northeast China. Sci. Total Environ. 803, 149871 https://doi.org/10.1016/J.SCITOTENV.2021.149871.

Zhang, Q., Wen, Q., Ma, T., Zhu, Q.H., Huang, D., Zhu, H., Xu, C., Chen, H., 2023. Cadmium-induced iron deficiency is a compromise strategy to reduce Cd uptake in rice. Environ. Exp. Bot. 206, 105155 https://doi.org/10.1016/J.ENVEXPBOT.2022.105155.

Zhang, H., Xie, S., Wan, N., Feng, B., Wang, Q., Huang, K., Fang, Y., Bao, Z., Xu, F., 2022. Iron plaque effects on selenium and cadmium stabilization in Cd-contaminated seleniferous rice seedlings. Environ. Sci. Pollut. Res. 1, 1–15. https://doi.org/10.1007/S11356-022-23705-2/FIGURES/5.

Zhang, J., Yang, N., Geng, Y., Zhou, J., Lei, J., 2019. Effects of the combined pollution of cadmium, lead and zinc on the phytoextraction efficiency of ryegrass (: Lolium perenne L.). RSC Adv. 9, 20603–20611. https://doi.org/10.1039/c9ra01986c.

Further reading

Kim, K.R., Owens, G., Naidu, R., 2010. Effect of root-induced chemical changes on dynamics and plant uptake of heavy metals in rhizosphere soils. Pedosphere 20 (4), 494–504.